Fundamental Understanding of Acid Gases Interaction With CeO_2: From Surface Science to Practical Catalysis

Uma Tumuluri[†], *Gernot Rother*[†] *and Zili Wu*[†‡*]

[†] Chemical Sciences Division, Oak Ridge National Laboratory, Oak Ridge, Tennessee, 37831.

[‡] Center for Nanophase Material Science, Oak Ridge National Laboratory, Oak Ridge, Tennessee, 37831.

ABSTRACT

Acid gases including CO_2, SO_2, and NO_x are ubiquitous in large scale energy applications including heterogeneous catalysis. The adverse environmental and health effects of these acid gases have gained high interest in the research and development of the technologies to remove or convert these acid gases. The main challenge for the development of these technologies is to develop catalysts that are highly efficient, stable and cost-effective and many catalysts have been reported in this regard. CeO_2 and CeO_2-based catalysts have gained prominence in the removal and conversion of CO_2, SO_2, and NO_x because of their structural robustness, redox and acid-base properties. In this paper, we provide a brief overview of the application of CeO_2 and CeO_2-based catalysts for CO_2, SO_2, NO_x gases removal with emphasis on the fundamental understanding of the interaction of these acid gases with CeO_2. The studies summarized in this review range from surface science using single crystals and thin films with precise crystallographic planes to practical catalysis applications of nanocrystalline and polycrystalline CeO_2 materials with defects and dopants. After an introduction into the properties of CeO_2 surfaces, their catalytic properties for conversions of different acid gases are reviewed and discussed. Surface atomic structure, oxygen vacancies, and surface acid-base property of CeO_2 play vital roles in the surface chemistry and structure evolution during acid gas interaction with CeO_2 and CeO_2-based catalysts.

INTRODUCTION

Acid gases such as CO_2, SO_2 and NO_x are pervasive in large scale energy applications.[1-6] A typical coal-fired power plant emits significant amount of CO_2, SO_2, NO_x gases.[3] These acid gases can also be present in many catalytic processes as reactants or products. The adverse impacts of these acid gases on the environment and global climate change have necessitated increased research interest with the goal of reducing harmful emissions. CO_2 can be removed by liquid amine scrubbing,[7-9] solid adsorbents[10-14] and polymer membranes.[15, 16] CO_2 can also be catalytically converted to useful chemicals via hydrogenation or via dry reforming of methane to make syngas.[17, 18] Dry and wet flue gas desulfurization and selective catalytic reduction (SCR) by NH_3 are the conventional processes used for SO_2 and NO_x removal. Many new catalysts have been developed for flue gas clean up to reduce the emissions of these pollutants,[1, 3, 4, 19-22] among which CeO_2, and CeO_2-based oxides are important candidates.

This paper presents a brief review of the application of CeO_2 and CeO_2-based catalysts in heterogeneous catalytic processes for the removal of CO_2, SO_2 and NO_x . CeO_2 is widely used in heterogeneous catalysis serving as both structural and electronic promoters.[23-31] CeO_2 has been used as a major component in three-way catalysts in the cleanup of automobile tailpipe emissions because of its high oxygen storage capacity.[23-26] The relative ease of switching between +4 and +3 oxidation states and the high oxygen storage capacity are considered as the key factors for the catalytic activity of CeO_2. However, these properties can be adversely impacted by the presence of acid gases even at low concentrations.[28]

To develop active, selective and stable catalysts for the removal and conversion of the acid gases, a prerequisite is to gain a fundamental understanding of how these gases interact with, and

convert, at the surface of the catalysts. The focus of this paper is to review the fundamental aspects governing this behavior, including surface speciation, conversion and regeneration from CO_2, NO_x, and SO_2 interactions. For each acid gas, the surface science work on ceria single crystals and thin films is presented first, followed by investigations on powder ceria in both single crystalline and polycrystalline forms, and finally studies via theoretical and computer modeling. This contribution is intended to complement other recent review articles, which cover broad ranges of surface chemistry studies on CeO_2-based materials, including surface science work[22, 32] as well as practical catalysis studies.[1-4, 19, 20, 28]

SURFACE STRUCTURES OF CERIA

Since the interaction of acid gases with CeO_2 starts with the gas adsorption on the surface of CeO_2, the surface structure of CeO_2 is deemed to be vital in determining catalytic activity. Hence it is helpful to briefly introduce the structure of some common CeO_2 surfaces before reviewing the catalysis research work. The three commonly observed CeO_2 facets, (111), (100), and (110), are shown in **Figure 1**, along with bulk CeO_2, which has fluorite structure. The coordination states of the surface cation, (Ce^{4+}), and anion (O^{2-}), differ on each surface. In bulk ceria, the coordination numbers of Ce and O are 8 and 4, respectively. As shown in **Figure 1**, on ceria (111), (100), and (110) surfaces, the coordination numbers for surface Ce^{4+} cations are 7, 6, 6, respectively, while the coordination numbers of the corresponding surface O^{2-} anions are 3, 2, and 3.[22, 33] The different surface atom arrangements and degrees of surface coordinative unsaturation (*cus*) of the cations and anions result in differences in oxygen vacancy formation energy, interaction strength with surface adsorbates, and thus different redox and acid-base

properties in forms of ceria single crystal, thin films,[22] or nanocrystalline ceria with defined surface planes.[34-38] It is generally believed that the (111), (110), and (100) facets dominate the surfaces of ceria nanocrystals, with morphologies of octahedra, rods, and cubes, respectively.

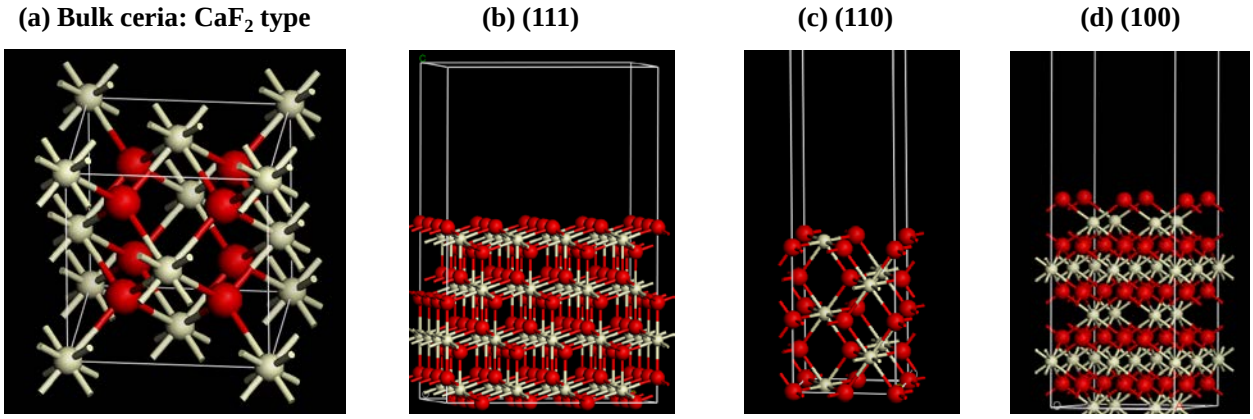

Figure 1: Structure of (a) bulk CeO_2, side view of (b) CeO_2 (111), (c) CeO_2 (110), and (d) CeO_2 (100).

CO_2 INTERACTION WITH CeO_2-BASED CATALYSTS

Surface science Studies of CO_2 on CeO_2 Surfaces: The interactions of CO_2 with CeO_2 model systems were studied by various groups.[18, 38-41] Senanayake and Mullins[39] observed that CO_2 interacts weakly with both oxidized and reduced CeO_2 (111) and observed similar behavior with a small amount of carbonate formed at low temperature that persisted up to 300 K on both surfaces. The interaction between CO_2 and reduced CeO_2 (111) surface was found much stronger than the stoichiometric CeO_2 (111) surface. CO_2 adsorption on oxidized CeO_2 (100) and partially reduced $CeO_{1.7}$ (100) thin films was investigated using soft X-ray photoelectron spectroscopy (sXPS), near-edge X-ray absorption fine structure (NEXAFS), Temperature programmed desorption (TPD) techniques and DFT calculations.[18] CO_2 adsorbed as carbonates (CO_3^{2-}) on both oxidized and partially reduced CeO_2 (100) films at 180 K. Coverage and

thermal stability of carbonates on partially reduced CeO_2 films are higher than the carbonates on the oxidized CeO_2 (100) films. DFT+U calculations were conducted on possible adsorption states for the carbonate and interestingly the most stable configuration was a tri-dentate species where the C in the CO_2 bonded to a surface O and the O in the CO_2 bonded in bridge sites to surface Ce. The reoxidation of the reduced CeO_{2-x}(100) surface by CO_2 was not observed. Staudt et al.[40] studied the interactions of CO_2 with CeO_{2-x} (111) films grown on Cu (111) single crystal surfaces using the resonant photoelectron spectroscopic technique. CO_2 was activated on intrinsic defect sites of CeO_2 surface at sufficiently high concentration of Ce^{3+} centers and partial reoxidation of CeO_{2-x} by CO_2 was observed at room temperature contradicting the results reported by Albrecht et al.[18] The deviation in the results reported by Staudt et al.[40] could be due to the fact that CeO_{2-x} (111) films were exposed to high doses of CO_2 (10 L, 200L, 4000 L, 10000 L and 20000 L CO_2 compared to 5L CO_2 exposure in the study reported by Albrecht et al.[18]) in their study. CO_2 adsorption on samples with different oxidation state (CeO_2/Cu, CeO_{2-x}/ Cu) and compositions (mixed MgO-CeO_2/Cu, MgO-CeO_{2-x}/Cu) was studied using scanning tunneling microscopy, and X-ray photoelectron spectroscopy techniques by Lykhach et al.[41] Carbonates and surface carboxylates were formed on CeO_2/Cu (stoichiometric and reduced) and MgO-CeO_2/Cu (stoichiometric and reduced) samples, and were similar to the species formed on polycrystalline CeO_2. Presence of MgO enhanced the formation of carbonate species, possibly due to the increase in the basicity caused by MgO in MgO-CeO_2/Cu samples which was also reported by Li et al.[30] . Interestingly, the reoxidation of Ce^{3+} to Ce^{4+} by CO_2 was suppressed by the presence of MgO due to formation of stable carbonates on Mg^{2+} sites, which did not undergo decomposition.

Extended to powder ceria but with well-defined surface planes as in the surface science counterparts, we recently studied CO_2 on CeO_2 nanoparticles (rods (defective surface), cubes (100), octahedra (111)) with well-defined facets using in situ IR spectroscopy coupled with mass spectrometry techniques.[38] CeO_2 rods, cubes and octahedra nanocrystals were prepared by hydrothermal treatment in Teflon-lined stainless steel autoclave.[42, 43] The surface structure of CeO_2 was controlled by varying the pH, temperature and duration of the reaction. CO_2 adsorbed in the form of bridged, monodentate, and bidentate carbonates (**Scheme I (a-c)**) and bicarbonates (**Scheme I (e)**) on all CeO_2 nanoparticles, however, the relative amount of carbonate species varied with the structure of CeO_2 nanoparticles. CeO_2 rods which are more defective bind CO_2 more strongly than the cubes and octahedra facets. The structure and binding strength of CO_2 were found to depend on the surface structure, reactivity of the surface oxygen and the presence of defects on CeO_2 nanoparticles.

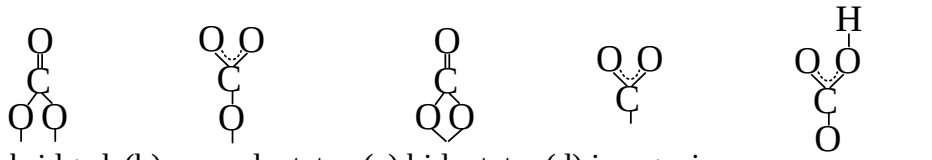

Scheme I: Structure of the adsorbed CO_2 on CeO_2. (a) bridged carbonate; (b) monodentate carbonate; (c) bidentate carbonate; (d) inorganic carboxylate; (e) bicarbonate.

Influence of synthesis procedures: Different synthesis procedure can lead to difference in surface property of the resulting ceria, such as amount and nature of defect sites. Consequently the interaction with CO_2 can be different for ceria synthesized via different procedures. Natile et al.[44] synthesized nanostructured CeO_2 powders by two different synthetic routes: (i) precipitation from a basic solution, and (ii) by a microwave-assisted heating hydrolysis method. CeO_2

particles prepared by the precipitation method have low surface area (41 m^2/g) with broad particle size distributions (8-15 nm) compared to the microwave-assisted method (72 m^2/g), which has smaller particles (3.3-4 nm). CeO_2 prepared by the microwave-assisted method is more reduced and adsorbs more CO_2 than the CeO_2 prepared by the precipitation method. The higher degree of reduction of the CeO_2 obtained by microwave-assisted method could be attributed to the smaller particles. Li et al.[45] studied CO_2 adsorption on CeO_2 nanorods (CeO_2-nanorods) synthesized by traditional hydrothermal synthesis[42] and the glycol solvothermal method (CeO_2-GST). CeO_2-GST exposing stable (111) facets have a larger number of oxygen vacancies than CeO_2-nanorods, which are exposed to (100) facet because of the reduction of glycol by valence change Ce^{4+} ' Ce^{3+}. CO_2 adsorbed in the form of bidentate and bridged carbonates and desorbed easily from the CeO_2-GSTsurface. However, CO_2 adsorbed in the form of monodentate and formate species on CeO_2-nanorods which are adsorbed more strongly compared to CeO_2-GST and could not be removed easily. CeO_2-GST, which has large number of vacancies, adsorbed more CO_2 (149 µmol/g) than CeO_2-rods (86 µmol/g). However, it is interesting to note that the even though the CeO_2-rods have less number of oxygen vacancies, it adsorbed CO_2 more strongly than the CeO_2-GST. High CO_2 binding strength observed in CeO_2-rods could be due to the adsorption of CO_2 on the more reactive (100) facet, compared to the stable (111) facet.

Mounfield et al.[46] investigated CO_2 interactions with traditionally prepared CeO_2-rods (hydrothermal synthesis) and metal organic framework (MOF) derived CeO_2 (MOF-CeO_2) to study the effect of morphology and coordination environment. CO_2 adsorbed in the form of bicarbonates, and monodentate carbonates on MOF-CeO_2, whereas, on CeO_2-rods, CO_2 adsorbs in the form of bidentate and monodentate carbonates. The MOF-CeO_2 exhibited higher CO_2

capture capacity (173.93 μmol/g) than the CeO_2-rods (130.65 μmol/g), presumably due to the retained porosity from the parent MOF and the inherent defects of MOF-CeO_2.

CO_2 adsorption studies on polycrystalline CeO_2 powders: CO_2 interaction with CeO_2 powders has been investigated extensively.[47-50] Bridged, monodentate, and bidentate carbonates and inorganic carboxylates (**Scheme I (a-d))** were observed during CO_2 adsorption on CeO_2[47-50] with the order of the thermal stability being: bridged carbonate < bidentate carbonate < inorganic carboxylate < monodentate carbonate.[47, 48] Yang et al.[51] prepared CeO_2 and Sm-CeO_2 using a space-confined method and investigated the effect of samarium (Sm) doping on CO_2 adsorption. The number of oxygen vacancies was increased by doping with samarium, which resulted in an increase in the CO_2 capture capacity (33.8 μmol/g for CeO_2; 99.1 μmol/g for Sm-CeO_2). The effects of dopants was also investigated recently by Li et al.[30] A series of high surface area CeO_2 and M-doped (M= Cu, La, Zr, and Mg) CeO_2 nanoparticles were prepared by a surfactant-template method and tested for their CO_2 capture properties. Of notice, the content of dopants is 4 mol% and thus the interaction of CO_2 with the materials is mostly via ceria surface. As shown in **Figure 2**, doping of CeO_2 with Cu or La increased the CO_2 capture capacity, whereas, doping of CeO_2 with Mg decreased the CO_2 capture capacity of CeO_2. Doping of CeO_2 with Zr had little effect on the CO_2 capture capacity. These changes were found to be related to the presence of surface defects on ceria. It was proposed that the relative amount of defect sites present on the surface of CeO_2 modified by dopants plays the vital role in CO_2 chemisorption while the defects induced in the bulk of CeO_2 are not directly involved.

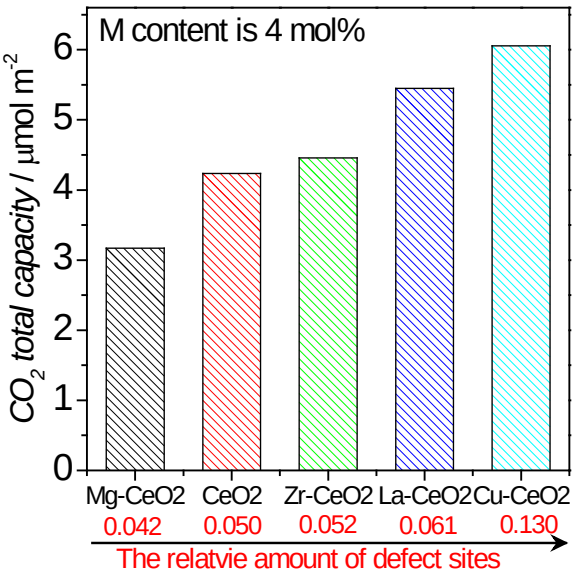

Figure 2: Effect of dopants on the CO_2 capture capacity of CeO_2.[30]

Theoretical Investigation of CO_2 Adsorption: CO_2 adsorption on model CeO_2 surfaces was investigated using density function theory (DFT) calculations by many research groups.[52-54] Hahn et al.[52] and Reimers et al.[53] studied the adsorption of CO_2 on CeO_2 (111) surface with DFT. Hahn et al.[52] reported that monodentate carbonate, bidentate carbonate and linear CO_2 species are formed, among which, the monodentate carbonates are most stable with a binding energy of -0.31 eV. A charge transfer of 0.46 e^- was calculated from CeO_2 (111) surface to the monodentate CO_2 species, indicating the basic character of CeO_2 (111) surface. At higher coverages (> 1/3 ML), multiple layers of linear CO_2 species adsorbed on top of monodentate carbonate mono layer, suggesting a weak interaction between linear CO_2 species and CeO_2 (111) surface.. Reimers et al.[53] observed the formation of planar CO_3^{2-} species during CO_2 adsorption on CeO_2 (111) and high adsorption energies were reported for CO_2 adsorption on CeO_2 (111) with O-vacancies compared to the stoichiometric CeO_2 (111) surfaces.

Cheng et al.[54] studied the adsorption and dissociation of CO_2 on the CeO_2 (110) surface. CO_2 adsorption and dissociation to CO on the stoichiometric and reduced CeO_2 (110) (both in-plane and split vacancy) were investigated via DFT. From the baseline repeating unit, CeO_2 (110) with an in-plane vacancy has one of the surface oxygens removed with little surface reconstruction. The split vacancy structure exhibits in-plane and out-of-plane movement of the remaining surface oxygen anion (O_v) so that it bridges with the surface cerium cations. The stoichiometric CeO_2 (110) exhibited weak CO_2 adsorption (physisorption) whereas, both reduced CeO_2 surfaces (in-plane and split oxygen vacancy) exhibited chemisorption. CO_2 adsorbed in the form of inorganic carboxylates on reduced CeO_2 with a split oxygen vacancy structure which are more stable than the monodentate carbonates formed on the CeO_2 with an in-plane oxygen vacancy. During the dissociation step, the inorganic carboxylates on reduced CeO_2 with in-plane oxygen vacancy were converted to bridged carbonate and then finally to CO whereas monodentate carbonates formed on CeO_2 with split oxygen vacancy were converted to asymmetric bidentate carbonate and the finally to CO. Adsorption of CO_2 resulted in the partial re-oxidation of the reduced CeO_2 surface. The experimental and computational studies performed on CeO_2 (100)[18] showed that CO_2 adsorbs solely in the form of tri-dentate planar carbonates and no carboxylate species were formed. CO_2 was the only reaction product and CO was not detected and no re-oxidation of the reduced CeO_2 (100) surface was observed.

In Summary, the presence of O vacancies plays a key role in the CO_2 interaction with CeO_2-based catalysts. The application of CeO_2 based adsorbent was not studied extensively in the literature. There were only 2 studies reported on the application of CeO_2 for CO_2 capture process. The CO_2 capture capacity of the CeO_2 catalysts can be enhanced by doping with metal cations, which increases the number of O vacancies. It has been reported that amine-based

sorbents adsorb more CO_2 in the presence of water vapor.[12, 55, 56] The increase in the CO_2 capture capacity might be due to the enhaced diffusion rates of physically bonded amine-water-CO_2 moieties.[56] The effect of humidity on the CO_2 adsorption performance of CeO_2-based catalysts has not been reported in the literature, which has to be investigated throughly for the application of CeO_2 for CO_2 capture process, since the flue gases contain water vapor.

NO_x INTERACTION WITH CeO_2-BASED CATALYSTS

Surface Science Studies of NO_x interaction with CeO_2: The wide use of ceria as a major component in NO removal catalysts inspired many studies of NO – CeO_2 interaction for understanding the reaction mechanism.[21, 57] Surface science work provides such kind of insights. Ferrizz et al.[58] observed that NO did not adsorb on oxidized CeO_2 (111) and CeO_2/±-Al_2O_3 (001) films at 300 K. Overbury et al.[59] also observed that NO did not adsorb on oxidized CeO_2 (001) surface either at 160 K or at 300 K. On slightly reduced CeO_2 (111) and CeO_2/±-Al_2O_3 (0001) surfaces, NO adsorbed molecularly at 300 K which dissociated into N_2 upon heating to 400 K resulting in the reoxidation of the reduced CeO_2 surface. NO dissociated on a highly reduced CeO_2 (111) surface and formed surface nitride species which were stable up to 400 K. Nitrides decomposed to N_2 at high temperatures (2 peaks at 475 and 625 K were observed). In contrast to the results reported by Ferrizz et al.,[58] reoxidation of CeO_{2-x}/Pt (111) after NO adsorption at 300 and 400 K was not observed by Berner et al.[60] The interaction of NO_2 with CeO_{2-x}/Pt (111) was also investigated by Berner et al.[60] NO_2 dissociated to NO adsorbates that occupy the two-fold bridging sites of Pt (111) at 300 and 400 K. Adsorption of NO_2 resulted in the reoxidation of Ce^{3+} to Ce^{4+}.

Overbury et al.[59] observed that NO adsorbed on sputtered (2 keV Ar^+ ions) CeO_2 (001) and on Rh/CeO_2 (001) films (Rh on both sputtered and oxidized CeO_2). NO adsorbed strongly on the Rh/sputtered CeO_2 (001) and had a higher desorption temperature than on sputtered CeO_2 (001) and RH/CeO_2 (001). The strong interaction between Rh and CeO_2 affects the reactivity with NO. Mullins et al.[61] investigated the decomposition of NO on Rh supported on oxidized and reduced CeO_2 films using soft X-ray photoelectron spectroscopy (SXPS). The degree and temperature of decomposition are reduced for Rh/reduced CeO_2 compared to the Rh/oxidized CeO_2 film. In another study, Overbury et al.[62] reported that NO did not adsorb on either oxidized CeO_2 (100) or CeO_2 (111) surface above 150 K but at 90 K NO adsorbed in the form of N_2O and nitrites. Whereas, on reduced CeO_2 surfaces, NO adsorbed in the form of NO^- and N_2O species. Various forms of N atoms ($N_{\pm}$, N^2, N^{3-}) were observed during NO adsorption and decomposition. On the reduced surfaces, the dissociation of NO occurred over a wide temperature range (150-300 K). Oxidation of reduced CeO_2 occurred upon adsorption at 90 K.

NO_x on CeO_2 nanocrystals: Very limited work was done with NO adsorption on ceria nanocrystals with well-defined surface facets as these nanocrystals have become available only in recent years. $MnO_x/Ce_{0.9}Zr_{0.1}O_2$ nanorods [63] showed excellent activity for SCR of NO with NH_3 at low temperature. $MnO_x/Ce_{0.9}Zr_{0.1}O_2$ exhibited 90% NO conversion at 423 K compared to $Ce_{0.9}Zr_{0.1}O_2$ nanorods (70% NO conversion at 623-703 K). According to the DFT calculations, Mn-CeO_2 (110) exhibited more feasibility for O-vacancy formation, faster nitrite formation, and higher NH_3 adsorption than the CeO_2 (110) model. Kawi et al.[64] investigated the effect of the structural and textural properties of CeO_2 on the selective catalytic reduction of NO_x with C_3H_6 and O_2. Hydrothermally (HT) prepared CeO_2 nanoparticles (surface area = 83.2 m^2/g) exhibited higher activity (60 % NO conversion) and stability in the presence of 10% water vapor

than the CeO_2 (30 % NO conversion) prepared by the precipitation (PP) method (37.8 m^2/g). Higher activity for NO reduction of HT CeO_2 nanoparticles was due to the high surface area, finer particles and high thermal stability.

NO_x interaction with polycrystalline CeO_2 powders: Zhang et al.[65] investigated the interaction of NO with commercial CeO_2 (Sigma Aldrich). NO adsorbed in the form of bidentate, monodentate, water-solvated, and bridging nitrates and *trans*-$N_2O_2^{2-}$ (1442 cm^{-1}) at 303 K on oxidized CeO_2. At higher temperatures (373- 573 K), formation of *cis*- $N_2O_2^{2-}$ species was observed. Whereas on reduced CeO_2, NO adsorbed in the form of bridging, bidentate, and monodentate nitrates, *trans*-$N_2O_2^{2-}$, *cis*- $N_2O_2^{2-}$, and NO^- species at 303 K (**Figure 3)**. IR absorbance intensity and thermal stability of NO-adsorbed species were found to be lower on reduced CeO_2 than the oxidized CeO_2. An interesting observation made by Zhang et al.[65] is that only surface NO_x-adsorbed species (*cis*- $N_2O_2^{2-}$) participate in the SCR of NO by NH_3 between 573 and 623 K. The nitrate species (monodentate, bidentate and bridged) formed during NO adsorption decompose as NO.

Contrary to the results reported by Zhang et al.,[65] Phillip et al.[66] and Symalla et al.[67] observed the formation of chelating nitrites along with a small amount of nitrates during NO adsorption on CeO_2. In the presence of O_2, the nitrites are oxidized to nitrates. Phillip et al.[66] also observed the formation of *trans*- and *cis*- $N_2O_2^{2-}$ species during NO adsorption on CeO_2 powder below 373 K and only *cis*- $N_2O_2^{2-}$ species above 373 K, similar to the results reported by Zhang et al.[65] In another study, Mihaylov et al.[68] reported the formation of surface azides (N_3^-) during adsorption of NO on reduced CeO_2 surfaces (supplied by Rodhia (France), and Daiichi Sankyo (Japan)), which was not reported anywhere else in the literature. Adsorption of NO on reduced CeO_2 led to the reoxidation of Ce^{3+} to Ce^{4+}.

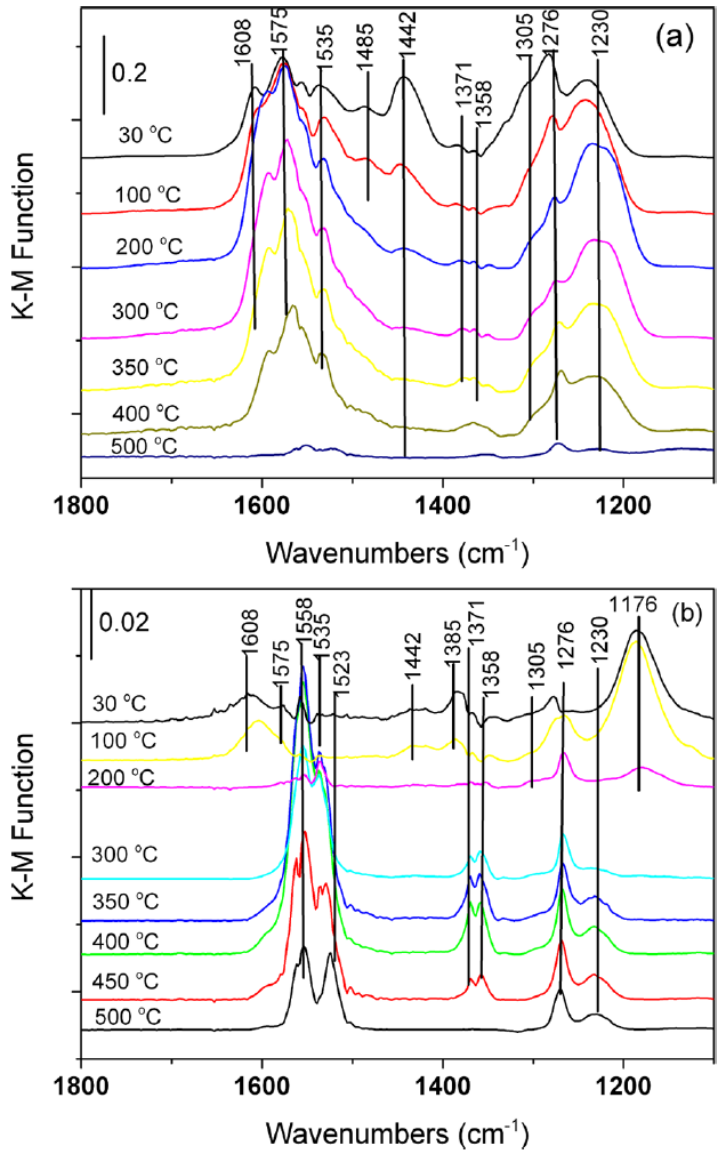

Figure 3: IR spectra during NO adsorption (500 ppm NO and balance He) at room temperature on (a) fully oxidized CeO_2 and (b) reduced CeO_2. The temperature was increased in He flow.[65]

Selective Catalytic Reduction of NO_x Using Mixed Oxides: Azambre et al.[69] investigated the NO and NO_2 interaction with commercial $Ce_xZr_{1-x}O_2$ mixed oxides. NO and NO_2 adsorbed in the form of nitrites and nitrates at 303 K. $Ce_xZr_{1-x}O_2$ mixed oxides adsorb more NO_2 than NO.

Nitrites and hyponitrites desorb at lower temperatures (below 523 K) than the nitrates (573-823 K). Gao et al.[70, 71] investigated the activities of CeO_2-TiO_2 catalysts for the selective catalytic reduction (SCR) of NO with NH_3 prepared by single step sol-gel, impregnation and co-precipitation method. Among the CeO_2-TiO_2 catalysts, the catalyst prepared by a single step sol-gel method exhibited the highest activity of SCR of NO because of the high surface area and high dispersion of nano-crystalline ceria. The CeO_2-TiO_2 catalyst prepared by the sol-gel method exhibited 98.6% NO conversion at SCR temperatures between 573 and 673 K. The NO conversion decreased to about 78% in 6 hours in the presence of 200 ppm SO_2 at 573 K. The NO conversion decreased from 70 to 50% in 4 hours when H_2O was introduced along with SO_2. However, at high reaction temperatures (623 K) the NO conversion showed less decrease (98.6 to 92.9%) in the presence of SO_2, which could be due to the decrease in the SO_2 binding strength on CeO_2-TiO_2 catalysts at high temperatures. Chen et al.[72] reported that the CuO-CeO_2-TiO_2 ternary oxide catalyst synthesized by a sol-gel method showed high SCR activity (>80 % at 423-473 K and about 100% at 523 K). CuO-CeO_2-TiO_2 exhibited higher activity (>80%) than the CeO_2-TiO_2 catalyst reported by Gao et al.[70, 71] CeO_2 enhances the surface area of the CuTi catalyst and leads to high dispersion of copper oxides on TiO_2 support, mainly in the form of isolated and coupled Cu^{2+}. Interaction of CeO_2 and CuO resulted in increased oxygen adsorption with high mobility. NH_3-SCR reaction on CuO-CeO_2-TiO_2 occurred between Cu^{+2}-NO, nitrate coordinated on CeO_2 sites and titanium sites bonded with NH_3.

Ma et al.[73] investigated the synergistic effects between CeO_2 and WO_x in the CeO_2-WO_x mixed oxide catalysts. WO_x/CeO_2 catalysts with different WO_x loadings prepared by a wet impregnation method were tested for the SCR activity. The CeO_2 catalyst with 10% WO_x loading gave a high SCR activity, 80% NO conversion over a wide temperature interval of 473-

673 K compared to CeO_2 (40 % NO conversion). A CeO_2-WO_x catalyst with Ce/W molar ratio of 3/2 (Ce_3W_2) synthesized by Chen et al.[74-76] exhibited high activity for NO reduction (100 % NO_x conversion at temperatures 473-723 K) compared to CeO_2 (70 % at 723 K), CeO_2/TiO_2 (90% at 573-673 K)[75, 76], or CeO_2-WO_x/TiO_2 (90% at 473-673 K)[75, 76] and high SO_2 tolerance. Ce_3W_2 catalyst maintained 100% NO conversion in the presence of 200 ppm SO_2 for 48 hr, whereas the NO conversion decreased from 90% to 35% for CeO_2/TiO_2 and from 90% to 67% for CeO_2-WO_x/TiO_2 catalysts. The strong interaction between Ce and W results in the increase in Ce^{3+} which led to the increase in the catalytic activity for SCR. Daturi et al.[77] reported that the deNO_x activity on the CeO_2 powders correlates with the ability of O vacancy formation. A $Ce_{0.75}Zr_{0.25}O_2$ catalyst with a larger number of oxygen vacancies (290 μmol/g catalyst) displayed higher activity for NO conversion (92%) than reduced CeO_2 (O vacancy: 90 μmol/g catalyst and NO conversion: 78%)

Ilieva et al. [78, 79] studied the reduction of NO by CO using a gold catalyst supported on CeO_2 and CeO_2-Al_2O_3 catalysts prepared by a co-precipitation method. An Au/CeO_2 (AuCe) catalyst exhibited higher NO conversion (78%) compared to Au/CeO_2-Al_2O_3 (51.5%) at 477 K. Addition of Al_2O_3 resulted in the increase in gold particle size, leading to the decrease in the catalytic activity. MnO_x-CeO_2 binary oxides were synthesized by Machida and coworkers[80] for adsorptive and subsequent reduction of NO_x (0.08% NO + 2% O_2) at low temperature (d 423 K). Chelating nitrites were formed during NO_x adsorption on MnO_x-CeO_2 and the nitrates decomposed to NO at 773 K.

Sn-modified MnO_x-CeO_2 catalysts with Sn:Mn:Ce = 1:4:5 prepared by Chang et al.[81] exhibited 100% NO_x conversion by NH_3 at 383-503 K compared to MnO_x-CeO_2 (86% at 383-503 K). Modification of MnO_x-CeO_2 with Sn resulted in the increase in the number of oxygen

vacancies and surface acidity which led to the enhancement of the SCR activity. The Sn-modified MnO_x-CeO_2 catalyst showed better tolerance towards SO_2 poisoning compared to the MnO_x-CeO_2 catalysts. In the presence of 100 ppm SO_2 and 9% H_2O, the NO conversion dropped to 62% at 383 K and 94% at 493 K for a Sn-modified MnO_x-CeO_2 catalyst, whereas for a MnO_x-CeO_2 catalyst the NO conversion dropped to 18% at 383 K and 56% at 493 K. MnO_x-CeO_2 supported on activated carbon honeycomb (MnO_x-CeO_2/ACH) catalysts showed high catalytic activities for selective catalytic reduction of NO with NH_3 at low temperatures.[82] The catalyst presented 100% NO conversion at 353 – 433 K and 98% NO conversion at 453-473 K. CeO_2 promotes the oxidation of NO and increases the amount of NO_3^- resulting in the enhancement of SCR activity of the MnO_x-CeO_2/ACH catalysts.

In H_2-SCR, 62.5 % NO conversion was reported for Pd/MnO_x-CeO_2 which was substantially higher than Pd/MnO_x (5.4 %) and Pd/CeO_2 (23.8 %) at 423 K by Machida et al.[80, 83, 84] Through a detailed study with XPS, TPD, and DRIFTS, a mechanism of reaction between adsorbed NO_x and H_2 was proposed and shown in **Figure 4**. The activated hydrogen formed on Pd migrates to the MnO_x-CeO_2 surface and reduces the oxide surface and nitrites (formed during NO sorption on MnO_x-CeO_2 surface) to form N_2 and H_2O. Costa et al. investigated the mechanistic aspects of the H_2-SCR of NO on Pt/Mg-CeO_2 catalysts which exhibited 83% nitrogen reaction selectivity and NO conversion between 80-97% in the presence of 5% H_2O and 20- 45 ppm SO_2 at 393-473 K.[85] NO_x is reduced by the active hydrogen formed at Pt surface, similar to the mechanism proposed by Machida et al.[83, 86]

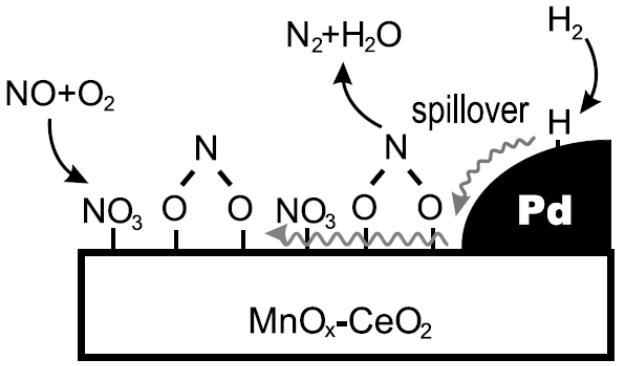

Figure 4: Possible mechanism for reaction of H_2 and NOx on Pd/MnO_x-CeO_2 catalyst.[86]

Rodriguez et al.[87] investigated the interaction of NO_2 with CeO_2 and MgO catalysts using synchrotron-based x-ray absorption near-edge spectroscopy, high resolution photoemission techniques and first-principles density functional calculations. NO_2 adsorbed in the form of thermally stable nitrates (NO_3^-) on CeO_2, which decomposed between 450 and 600 K. NO_3^- and adsorbed NO_2 were the main species that were formed during NO_2 adsorption on a MgO catalyst. NO_2 interacted strongly with MgO and the adsorbed species decomposed at higher temperatures (600-800 K) than the adsorbed species on CeO_2.

Theoretical Investigation of NO_x Adsorption: Yang et.al., investigated the adsorption of NO on stoichiometric and reduced CeO_2 (111) and (110) surfaces using DFT theory within the generalized gradient approximation.[88] On a stoichiometric CeO_2 (111) surface the most preferred mode of NO adsorption was atop the Ce site with adsorption energy of 2.33 kcal/mol, whereas on a stoichiometric CeO_2 (110) surface, the most preferred adsorption modes were Ce_x-bridge modes. On reduced CeO_2 surfaces the optimized structure was the tilted structure with O atom closest to the substrate. The adsorption of NO on reduced CeO_2 surfaces was stronger than on the oxidized surfaces. In another DFT+U study on NO adsorption on a reduced CeO_2 (110) surface the formation of NO_2 with nearby lattice O was observed.[89] NO_2 then dissociated into

NO and O to fill the original O vacancy. 2 or more adsorbed NO molecules adsorbed at isolated O vacancies could also combine to form N_2O_2 which dissociates to N_2. Nolan et al.[90] investigated the adsorption of NO_2 on reduced ceria (111), (110) and (100) surfaces with DFT+U calculations. NO_2 was converted to NO on reduced CeO_2 surfaces. Adsorption of NO_2 on defective CeO_2 surfaces resulted in some reoxidation of Ce^{3+}, with an electron being transferred to NO_2 to form NO_2^- as an intermediate. The conversion of NO_2 to NO was more favorable on the (111) surface than on the (110) and (100) surfaces as the O vacancy in (111) is least stable on the (111) surface.

To sum up this section, it has been shown that the surface area, particle size of and number of oxygen vacancies in the ceria and ceria-based catalyst play a vital role in the SCR of NOx gases. In situ IR studies show that nitrates/nitrites are formed during NO adsorption on CeO_2, however the structure of adsorbed NO_x is still ambiguous. Some studies reported the formation of nitrates while other reported the formation of nitrites. CeO_2 catalysts with high activity (98-100% NO_x conversion) for NO_x reduction have been reported, however these catalysts were not tested in the actual flue gas conditions which contains trace amounts of SO_2 and H_2O. Only a few studies investigated the effect of SO_2 and H_2O on the catalytic activity for NO_x reduction and reported that the catalytic activity decreases in the presence of SO_2 and H_2O. Studies on the effect of long term exposure of SO_2 and H_2O on the catalytic activity of CeO_2 and CeO_2–based catalysts are important for the design of SO_2-resistant catalysts.

SO_2 INTERACTION WITH CeO_2-BASED CATALYSTS

Due to the detrimental effect of trace SO_2 in various processes on the performance of CeO_2 and CeO_2-based catalysts, numerous studies have been devoted to study SO_2 interaction with pure CeO_2 and CeO_2-based catalysts using various characterization techniques such as IR and Raman spectroscopy, X-ray photoemission spectroscopy (XPS) and X-ray absorption near-edge spectroscopy (XANES).

Surface Science Studies of SO_2 on CeO_2: Overbury et al.[91] investigated the interaction of SO_2 with oxidized and reduced CeO_2 (111) films (< 5 nm) on Ru (0001) substrate using soft X-ray photoelectron spectroscopy (SXPS), and thermal desorption spectroscopy. SO_2 adsorbed as sulfites on oxidized CeO_2 films at temperature below 300 K which is consistent with the previously reported studies.[92] However, the reduction of CeO_2 surface, as reported in the literature,[93-96] was not observed. The sulfites were strongly bound to the CeO_2 surface and some were stable even at high temperature (600 K). On the reduced CeO_2(111) film, sulfites were formed upon SO_2 exposure at temperatures below 300 K, and the sulfite species were converted to sulfides at temperatures above 300 K. Contradictory to other results reported in the literature,[93-97] the XPS results showed that the ratio of Ce^{4+}/Ce^{3+} increased on reduced CeO_2 films after exposure to SO_2 followed by annealing, indicating that the surface was oxidized after SO_2 adsorption. In another study, Happel et al.[98] investigated SO_2 adsorption on stoichiometric and reduced CeO_2 (111) films supported on Cu (111) using synchrotron radiation photoelectron spectroscopy (SR-PES). Similar to the results reported by Overbury et al.,[91] the authors observed that sulfites were the predominant species formed upon adsorption of SO_2 on both stoichiometric and reduced CeO_2 films at 300 K, however sulfates were formed at higher adsorption temperatures (above 400 K). Surface sulfides (S^{2-}) were formed during decomposition, and the formation of sulfides was observed at lower temperatures (300 K) on a

reduced CeO_2 film compared to the stoichiometric CeO_2 (400 K). At temperatures above 550 K the surface sulfides were converted to bulk sulfides. The interaction of stoichiometric CeO_2 (111) with SO_2 resulted in a minor change of the Ce oxidation state, whereas interaction of SO_2 with reduced CeO_2 (111) film led to strong reoxidation of Ce, similar to the results reported by Overbury et al.[91] Happel et al.[99] also investigated the mechanism of SO_2 decomposition on a Pt/CeO_2 (111) model catalyst. The adsorbed species formed on Pt/CeO_2 and CeO_2 during SO_2 adsorption are similar. However, during annealing at temperatures between 300 and 500 K, the surface species were converted to atomic sulfur located mainly on Pt particles and this process led to the reoxidation of CeO_2 due to the liberation of oxygen.

Ferriz at al.,[93] studied the SO_2 interaction with polycrystalline CeO_2 thin films supported on titanium foil and on Mo(100) using XPS and temperature-programmed desorption (TPD). They reported that the adsorption of SO_2 on CeO_2 thin films at 298 K resulted in the formation of molecularly adsorbed SO_2 and small amounts of sulfate species. The adsorbed SO_2 desorbed and re-adsorbed as surface sulfate species when heated to higher temperatures (373 to 673 K). High concentrations of surface sulfates were produced when the CeO_2 film was heated to 573 K in the presence of $SO_2 + O_2$. The XPS results are in agreement with results reported by Waqif et al.[92] on polycrystalline CeO_2 powder especially at high temperatures. However, Ferriz et al. did not observe the formation of sulfite species at room temperature as reported by Waqif et al.[92] Adsorption of SO_2 results in the partial reduction of the CeO_2 surface, which is in agreement with the results (on polycrystalline CeO_2 powder) reported by Flouty et al.[94] In another study, Rodriguez et al.[100] evaluated the SO_2 adsorption on pure and reduced CeO_2 powders and thin films (3-4 nm thick) using synchrotron-based high-resolution photoemission, X-ray absorption near-edge spectroscopy (XANES) and TPD. XANES showed the formation of sulfates on both

CeO_2 powder and thin films when exposed to SO_2 at 300 K, which is contrary to the results reported by Waqif et al.[92] The sulfate species decomposed to SO_2 and some SO_3 species at temperatures in the range of 390 – 670 K. It was also reported that the formation of sulfites is favored when O-vacancies are introduced on the CeO_2 surface.

SO_2 interaction with CeO_2 nanocrystals In our recent work,[101] we investigated the adsorption and reaction of SO_2 on three CeO_2 nanocrystals: rods (defective structure), cubes (100) and octahedra (111) in both pre-oxidized and pre-reduced states. The nature, strength and amount of SOx species formed from SO_2 adsorption were found dependent on the surface structure of CeO_2 nanocrystals. SO_2 adsorbed in the form of surface sulfates and sulfites on CeO_2 rods, cubes and octahedra in both pre-oxidized and pre-reduced states. Surface sulfites were more prominent on CeO_2 octahedra than the other two surfaces while surface sulfate species were the most favored on CeO_2 rods. Bulk sulfite species were also formed on pre-reduced CeO_2 rods in addition to surface sulfites and sulfates. Differences in the SO_2 interaction with CeO_2 nanoshapes are due to the differences in the reactivity of the surface oxygen and number of defect sites. CeO_2 rods, which have high basicity and large amount of defects, bind SO_2 more strongly than CeO_2 cubes and octahedra nanocrystals. The adsorbed SO_x species on CeO_2 rods desorbed at higher temperature than on the CeO_2 cubes and octahedra (**Figure 5**). CeO_2 octahedra desorbed slightly more SO_2 (2.42 μ mol/m^2) than cubes (2.07 μ mol/m^2) but significantly more than rods (0.45 μ mol/m^2). SO_2 binding strength on CeO_2 rods and cubes was higher than octahedra and not all of the adsorbed SO_x species completely desorbed during TPD, especially on rods.

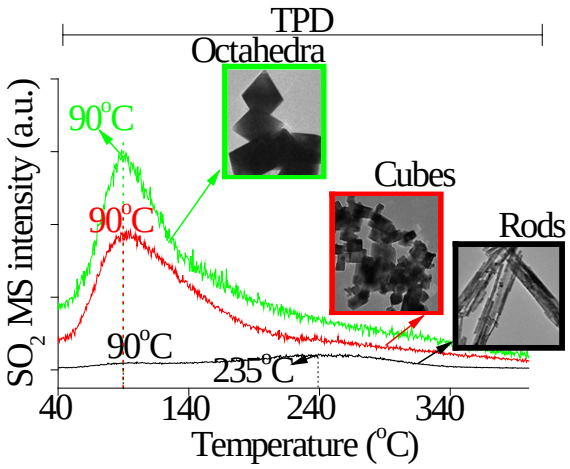

Figure 5: TPD profiles following room temperature SO_2 adsorption on CeO_2 rods, cubes, and octahedra.

SO_2 interaction with polycrystalline CeO_2: Waqif et al.[92, 102] studied the SO_2 adsorption on commercial CeO_2 powders (provided by Rhône Poulenc) with different surface areas using gravimetric sorption and IR spectroscopy. Both surface and bulk sulfates were formed during SO_2 adsorption and the degree of the formation of these species depends on the surface area of the CeO_2 sample, SO_2 concentration and adsorption temperature. Bulk sulfates were favored at high SO_2 concentration, high adsorption temperature (above 373 K), and low surface area of CeO_2 sample. The surface sulfate species were persistent and present on the CeO_2 sample even after evacuation at 973 K, whereas a large part of bulk species desorbed at 873 K. In another work, Bazin et al.[103] investigated the effect of platinum on the sulfation of ceria and found that the presence of platinum had no effect on the structure and thermal stability of the sulfate species formed during SO_2 adsorption. Lavelley[104] also observed the formation of surface sulfates at temperature above 373 K. Sulfite species were formed at adsorption temperatures below 373 K. Similar to the results reported by Waqif et al.[92, 102] and Lavelley[104], formation of surface sulfites

during SO_2 adsorption on Pd/CeO_2 at temperatures between 298 and 473 K was also observed by Luo et al.[105]

Flouty et al.[94] investigated the SO_2 adsorption on CeO_2 prepared by a precipitation method using $Ce(NO)_3.6H_2O$ and NaOH. The adsorption of SO_2 on the CeO_2 was studied using thermal analysis, Raman spectroscopy, and electron paramagnetic resonance (EPR) techniques. Contradictory to the results reported by Waqif et al.[92] and Lavelley,[104] Flouty et al. reported that only sulfates formed at room temperature. A concomitant reduction of Ce^{4+} to Ce^{3+} was also observed during CeO_2 sulfation. Twu et al.[106] observed the formation of surface pyrosulfates ($S_2O_7^{2-}$) and bulk sulfates at temperatures above 623 K in their Raman studies of sulfation of CeO_2.

SO_2 interaction with Mixed Oxides: The synergistic effect of mixed catalysts of CeO_2 and MgO on the SO_2 oxidation and adsorption was investigated by Jiang et al.[107]. The SO_2 adsorption performance of the CeO_2-MgO mixtures with different crystal sizes was evaluated using a gravimetric sorption method. The SO_2 pickup rate and capture capacity of the CeO_2-MgO mixed oxides (1.7 g/g) were significantly higher than those of pure CeO_2 (0.29 g/g) and MgO (0.26 g/g). The crystal size of the CeO_2 and MgO has a significant effect on the SO_2 sorption activity, which includes SO_2 pick up rate and capacity. The SO_2 interaction with CeO_2-ZrO_2 mixed catalysts was investigated by FTIR, pulse-reactor and TPD by Luo et al.[108]. SO_2 adsorbed mainly in the form of bulk sulfates at 473 K, whereas on ZrO_2 surface sulfates are formed upon SO_2 exposure and the amount of sulfates increases with the increase in the Ce content in the mixed oxides. In another study, Yu et al.[109] reported that a $CeO_2/^3$-Al_2O_3 sorbent prepared by wet impregnation of $Ce(NO_3)_3.6H_2O$ on ^{3}-Al_2O_3 (surface area = 277.8 m^2/g)

exhibited good regeneration performance over 3 cycles. The reaction order with respect to SO_2 was reported as first order.

Theoretical calculations: Apart from the numerous experimental studies, theoretical studies of SO_2 adsorption on CeO_2 were also performed by Lu et al.[110, 111] and Kullgren et al.[112] who investigated the sulfidation and sulfation of CeO_2 (111) and (110) surfaces in oxidizing and reducing conditions based on density functional theory (DFT) calculations. Sulfates were prominent on both oxidized (111) and (110) surfaces. Surface sulfates were more stable on reduced (110) surface, whereas sulfides were more stable on reduced (111) surface. Liu et al.[113] investigated the SO_2 interaction with CeO_2 (111) and Mn-doped CeO_2 (111) by DFT calculations along with ab initio thermodynamics method. Sulfates and sulfites were the stable species formed during SO_2 interaction with the CeO_2 (111) surface. The sulfites were converted into sulfates upon heating with and without the presence of oxygen. The sulfates formed on Mn-doped CeO_2 were more stable and require higher temperature (about 160 K higher) to dissociate than the sulfates formed on pure CeO_2 surface. Doping with Mn resulted in the increase in the number of defects, which act as a Lewis base site and adsorbed SO_2 more strongly than the pure CeO_2 surface.

SO_2 adsorption on stoichiometric and reduced CeO_2 (100) surface was conducted in our recent work[101] using DFT calculations. Sulfites, chemisorbed SO_2 and sulfates were prominent on the stoichiometric CeO_2 (100) surface and sulfites were favored on the reduced CeO_2 (100) surface. The S-O bond length of sulfite species closest to the surface oxygen ($S\text{-}O_{surf}$) is slightly longer than the sulfate species on the pristine CeO_2 (100). The large O-O distance (3.71 Å)[114] in pristine (100) is not favorable for the formation of sulfate species, however the low O vacancy

formation energy (2.27eV compared to 2.600 eV for (111) surface)[115] of (100) surface allows the formation of the sulfate species.

In summary, the interaction of SO_2 with CeO_2 has been studied intensively and provided fundamental insights on the reaction mechanism during SO_2 adsorption. The main focus of these studies was to investigate the species formed during SO_2 adsorption. However, there is a serious lack of studies which focus on the binding strength of the sulfate/sulfite species that are formed upon SO_2 adsorption. For practical applications, the catalysts should be able to regenerate completely after SO_2 adsorption. The past studies show that the sulfates/sulfites on CeO_2 and CeO_2 –based catalysts are stable at temperatures above 623 K. More studies should be performed to investigate the regenerability and ways to improve it for CeO_2 and CeO_2-based catalysts so that they can be used as sulfur-resistant catalysts and possible sorbents for multiple SO_2 capture cycles.

SUMMARY AND OUTLOOK

This paper gave a brief overview of the fundamental studies of the interactions of acid gases CO_2, NOx and SO_2 with ceria and ceria-based catalysts using various techniques such as in situ IR, Raman spectroscopy, XPS, TPD, and XAFS etc, complemented with theoretical work. From the broad range of work from science surface to practical catalysis, it becomes clear that the surface structure, the presence of surface oxygen vacancies, the reactivity of the surface oxygen, surface acidity and basicity play a vital role in determining the interaction of CO_2, SO_2 and NO_x with CeO_2-based catalysts. Some contradictions in the literature on how the acid gases interact with ceria-based catalysts among different research groups may reflect the differences in these properties of the ceria catalysts. Overall, these investigations provide some insights for designing

more effective and stable catalysts in reactions and processes involved with these acid gases. For example, to enhance the CO_2 and SO_2 adsorption capacity and catalytic activity of NO reduction over CeO_2 and CeO_2-based sorbents/catalysts, one may do so by doping with metal cations which introduces more vacancies into ceria while also enhancing the stability and robustness of ceria.

Despite of the extensive number of techniques used in characterizing the interaction between acid gases and ceria and ceria-based materials, it still remains unclear how the bulk defects and lattice oxygen in ceria play a role in interacting with acid gases especially at higher temperatures when bulk species can form and catalyst deactivation happens. This question may be answered by advanced techniques such as neutron scattering. Neutron diffraction (ND) is a powerful tool in characterizing the structure of oxides, providing quantitative, average structural (lattice parameter), and microstructural (domain size, lattice strain, defects) information under in situ reaction conditions.[116] Neutrons are better at 'seeing' oxygen than x-rays. The property of structural defects in ceria was quantified using neutron diffraction with Rietveld analysis.[117 118] Vacancies, displacement, and addition of extra atoms in the oxygen sub-lattice can be identified by careful examination of the pair distribution function (PDF) data, especially if advanced modeling techniques are utilized. We expect that by studying the acid gases interaction with ceria, particularly the uniform and well-structured nanoshapes, via in situ ND, the dynamics of the defects and strains in ceria can be obtained and will provide a better understanding of how the bulk defects influence the interaction with acid gases.

Since the co-existence of the various acid gases is general and often time moisture is present, future studies of how ceria and ceria-based catalysts perform in the presence of multiple acid gases should be carried out to derive parameters for designing more resilient catalysts for

practical usage. For example, the studies reported in literature mainly focus on obtaining the fundamental insights on the interaction ofCeO_2 with individual acid gas. However, these catalysts were not tested in the real flue gas environments which contain a mixture of CO_2, SO_2, H_2O, and NO_xthat may greatly influence the surface chemistry and catalytic behaviors of CeO_2-based catalysts. Although CeO_2-based catalysts exhibit high NO_x conversion and N_2 selectivity, there are only few studies that investigated the effect of SO_2 and H_2O on the NO conversion. CeO_2-based catalysts exhibit strong interaction with SO_2 and regeneration capacity of these catalysts after SO_2 exposure was not thoroughly investigated, which is a vital aspect for the development of more stable catalysts. Ceria and ceria-based catalysts in the form of nanocrystals with well-defined surface structures can be nice models for achieving fundamental understanding of how the practical catalysts behave in the complex environment containing mixtures of various acid gases.

AUTHOR INFORMATION

Corresponding Author

*Email: wuz1@ornl.gov. Telephone: 865-576-1080

Funding Sources

U.S. Department of Energy, Office of Science, Basic Energy Sciences.

ACKNOWLEDGEMENTS

This work is supported by the Center for Understanding and Control of Acid Gas-Induced Evolution of Materials for Energy (UNCAGE-ME), an Energy Frontier Research Center funded

by U.S. Department of Energy, Office of Science, Basic Energy Sciences. This contribution was identified by Session Chair Dr. Sanjaya Senanayake (Brookhaven National Laboratory) as the Best Presentation in the session “Advances in Ceria Based Catalysis: Structural, Electronic and Chemical Properties Tailored for Chemical Conversion” of the 2015 ACS Fall National Meeting in Boston, MA.

REFERENCES

1. Skalska, K.; Miller, J. S.; Ledakowicz, S., Trends in NO_x abatement: A review. *Sci. Total Environ.* **2010**, *408*, 3976.
2. Hamada, H.; Haneda, M., A review of selective catalytic reduction of nitrogen oxides with hydrogen and carbon monoxide. *Appl. Catal. A: Gen.* **2012**, *421-422*, 1.
3. Liu, Y.; Bisson, T. M.; Yang, H.; Xu, Z., Recent developments in novel sorbents for flue gas clean up. *Fuel Proc. Tech.* **2010**, *91*, 1175.
4. Mathieu, Y.; Tzanis, L.; Soulard, M.; Patarin, J. l.; Vierling, M.; MoliÃ¨re, M., Adsorption of SO_x by oxide materials: A review. *Fuel Proc. Tech.* **2013**, *114*, 81.
5. Wang, J.; Huang, L.; Yang, R.; Zhang, Z.; Wu, J.; Gao, Y.; Wang, Q.; O'Hare, D.; Zhong, Z., Recent advances in solid sorbents for CO_2 capture and new development trends. *Energy Environ. Sci.* **2014**, *7*, 3478.
6. Jones, C. W., CO_2 capture from dilute gases as a component of modern global carbon management. *Annu. Rev. Chem. Biomol. Eng.* **2011**, *2*, 31.
7. Yang, J.; Yu, X.; Yan, J.; Tu, S.-T., CO_2 Capture Using Amine Solution Mixed with Ionic Liquid. *Ind. Eng. Chem. Res.* **2014**, *53*, 2790.
8. Mandal, B. P.; Guha, M.; Biswas, A. K.; Bandyopadhyay, S. S., Removal of carbon dioxide by absorption in mixed amines: modelling of absorption in aqueous MDEA/MEA and AMP/MEA solutions. *Chem. Eng. Sci.* **2001**, *56*, 6217.
9. Hagewiesche, D. P.; Ashour, S. S.; Al-Ghawas, H. A.; Sandall, O. C., Absorption of carbon dioxide into aqueous blends of monoethanolamine and N-methyldiethanolamine. *Chem. Eng. Sci.* **1995**, *50*, 1071.
10. Arenillas, A.; Smith, K. M.; Drage, T. C.; Snape, C. E., CO_2 capture using some fly ash-derived carbon materials. *Fuel* **2005**, *84*, 2204.
11. Arstad, B.; Fjellvåg, H.; Kongshaug, K. O.; Swang, O.; Blom, R., Amine functionalised metal organic frameworks (MOFs) as adsorbents for carbon dioxide. *Adsorption* **2008**, *14*, 755.
12. Belmabkhout, Y.; Serna-Guerrero, R.; Sayari, A., Adsorption of CO_2-Containing Gas Mixtures over Amine-Bearing Pore-Expanded MCM-41 Silica: Application for Gas Purification. *Ind. Eng. Chem. Res.* **2010**, *49*, 359.
13. Bezerra, D. g. P.; Silva, F. W. M. d.; Moura, P. A. S. d.; Sousa, A. G. S.; Vieira, R. S.; Rodriguez-Castellon, E.; Azevedo, D. C. S., CO_2 adsorption in amine-grafted zeolite 13X. *Appl. Surf. Sci.* **2014**, *314*, 314.

14. Chaikittisilp, W.; Khunsupat, R.; Chen, T. T.; Jones, C. W., Poly(allylamine)-mesoporous silica composite materials for CO_2 capture from simulated flue gas or ambient air. *Ind. Eng. Chem. Res.* **2011**, *50*, 14203.
15. Azzouz, A.; Platon, N.; Nousir, S.; Ghomari, K.; Nistor, D.; Shiao, T. C.; Roy, R., OH-enriched organo-montmorillonites for potential applications in carbon dioxide separation and concentration. *Sep. Purif. Technol.* **2013**, *108*, 181.
16. Wang, X.; Min, M.; Liu, Z.; Yang, Y.; Zhou, Z.; Zhu, M.; Chen, Y.; Hsiao, B. S., Poly(ethyleneimine) nanofibrous affinity membrane fabricated via one step wet-electrospinning from poly(vinyl alcohol)-doped poly(ethyleneimine) solution system and its application. *J. Membr. Sci.* **2011**, *379*, 191.
17. Pakhare, D.; Spivey, J., A review of dry (CO_2) reforming of methane over noble metal catalysts. *Chem. Soc. Rev.* **2014**, *43*, 7813.
18. Albrecht, P. M.; Jiang, D.-e.; Mullins, D. R., CO_2 Adsorption As a Flat-Lying, Tridentate Carbonate on CeO_2(100). *J. Phys. Chem. C* **2014**, *118*, 9042.
19. Rezaei, F.; Rownaghi, A. A.; Monjezi, S.; Lively, R. P.; Jones, C. W., SO_x/NO_x Removal from Flue Gas Streams by Solid Adsorbents: A Review of Current Challenges and Future Directions. *Energy Fuels* **2015**, *29*, 5467.
20. Roy, S.; Hegde, M. S.; Madras, G., Catalysis for NO_x abatement. *Appl. Energy* **2009**, *86*, 2283.
21. Liu, F.; Yu, Y.; He, H., Environmentally-benign catalysts for the selective catalytic reduction of NOx from diesel engines: structure-activity relationship and reaction mechanism aspects. *Chem. Commun.* **2014**, *50*, 8445.
22. Mullins, D. R., The surface chemistry of cerium oxide. *Surf. Sci. Rep.* **2015**, *70*, 42.
23. Kašpar, J.; Fornasiero, P.; Graziani, M., Use of CeO_2-based oxides in the three-way catalysis. *Catal. Today* **1999**, *50*, 285.
24. Farrauto, R. J.; Heck, R. M., Catalytic converters: state of the art and perspectives. *Catal. Today* **1999**, *51*, 351.
25. Trovarelli, A.; de Leitenburg, C.; Boaro, M.; Dolcetti, G., The utilization of ceria in industrial catalysis. *Catal. Today* **1999**, *50*, 353.
26. Kašpar, J.; Fornasiero, P.; Hickey, N., Automotive catalytic converters: current status and some perspectives. *Catal. Today* **2003**, *77*, 419.
27. Melchionna, M.; Fornasiero, P., The role of ceria-based nanostructured materials in energy applications. *Mater. Today* **2014**, *17*, 349.
28. Trovarelli, A., Catalytic Properties of Ceria and CeO_2-Containing Materials. *Catal. Rev.* **1996**, *38*, 439.
29. Flytzani-Stephanopoulos, M., Nanostructured Cerium Oxide "Ecocatalysts". *MRS Bulletin* **2001**, *26*, 885.
30. Li, M.; Tumuluri, U.; Wu, Z.; Dai, S., Effect of Dopants on the Adsorption of Carbon Dioxide on Ceria Surfaces. *ChemSusChem* **2015**, *8*, 3651.
31. Rodriguez, J. A.; Hrbek, J., Interaction of Sulfur with Well-Defined Metal and Oxide Surfaces: Unraveling the Mysteries behind Catalyst Poisoning and Desulfurization. *Acc. Chem. Res* **1999**, *32*, 719.
32. Paier, J.; Penschke, C.; Sauer, J., Oxygen Defects and Surface Chemistry of Ceria: Quantum Chemical Studies Compared to Experiment. *Chem. Rev.* **2013**, *113*, 3949.

33. Ganduglia-Pirovano, M. V.; Hofmann, A.; Sauer, J., Oxygen vacancies in transition metal and rare earth oxides: Current state of understanding and remaining challenges. *Surf. Sci. Rep.* **2007**, *62*, 219.
34. Qiao, Z. A.; Wu, Z. L.; Dai, S., Shape-Controlled Ceria-based Nanostructures for Catalysis Applications. *ChemSusChem* **2013**, *6*, 1821.
35. Wu, Z. L.; Li, M. J.; Overbury, S. H., On the structure dependence of CO oxidation over CeO_2 nanocrystals with well-defined surface planes. *J. Catal.* **2012**, *285*, 61.
36. Wu, Z.; Li, M.; Mullins, D. R.; Overbury, S. H., Probing the Surface Sites of CeO_2 Nanocrystals with Well-Defined Surface Planes via Methanol Adsorption and Desorption. *ACS Catal.* **2012**, *2*, 2224.
37. Wu, Z. L.; Li, M. J.; Howe, J.; Meyer, H. M.; Overbury, S. H., Probing Defect Sites on CeO_2 Nanocrystals with Well-Defined Surface Planes by Raman Spectroscopy and O_2 Adsorption. *Langmuir* **2010**, *26*, 16595.
38. Wu, Z.; Mann, A. K. P.; Li, M.; Overbury, S. H., Spectroscopic Investigation of Surface-Dependent Acid–Base Property of Ceria Nanoshapes. *J. Phys. Chem. C* **2015**, *119*, 7340.
39. Senanayake, S. D.; Mullins, D. R., Redox Pathways for HCOOH Decomposition over CeO_2 Surfaces. *J. Phys. Chem. C* **2008**, *112*, 9744.
40. Staudt, T.; Lykhach, Y.; Tsud, N.; SkÃ¡la, T.; Prince, K. C.; MatolÃn, V.; Libuda, J., Ceria reoxidation by CO_2: A model study. *J. Catal.* **2010**, *275*, 181.
41. Lykhach, Y.; Staudt, T.; Streber, R.; Lorenz, M. P. A.; Bayer, A.; SteinrÃck, H. P.; Libuda, J., CO_2 activation on single crystal based ceria and magnesia/ceria model catalysts. *EPJ B* **2010**, *75*, 89.
42. Mai, H.-X.; Sun, L.-D.; Zhang, Y.-W.; Si, R.; Feng, W.; Zhang, H.-P.; Liu, H.-C.; Yan, C.-H., Shape-Selective Synthesis and Oxygen Storage Behavior of Ceria Nanopolyhedra, Nanorods, and Nanocubes. *J. Phys. Chem. B* **2005**, *109*, 24380.
43. Yan, L.; Yu, R.; Chen, J.; Xing, X., Template-Free Hydrothermal Synthesis of CeO_2 Nano-octahedrons and Nanorods: Investigation of the Morphology Evolution. *Cryst. Growth Des.* **2008**, *8*, 1474.
44. Natile, M. M.; Boccaletti, G.; Glisenti, A., Properties and Reactivity of Nanostructured CeO_2 Powders: Comparison among Two Synthesis Procedures. *Chem. Mater.* **2005**, *17*, 6272.
45. Li, C.; Liu, X.; Lu, G.; Wang, Y., Redox properties and CO_2 capture ability of CeO_2 prepared by a glycol solvothermal method. *Chin. J. Catal.* **2014**, *35*, 1364.
46. Mounfield Iii, W. P.; Tumuluri, U.; Jiao, Y.; Li, M.; Dai, S.; Wu, Z.; Walton, K. S., Role of Defects and Metal Coordination on Adsorption of Acid Gases in MOFs and Metal Oxides: An In Situ IR Spectroscopic Study. *Micropo. Mesopor. Mater.* **2016**, *227*, 65.
47. Li, C.; Sakata, Y.; Arai, T.; Domen, K.; Maruya, K.-i.; Onishi, T., Carbon monoxide and carbon dioxide adsorption on cerium oxide studied by Fourier-transform infrared spectroscopy. Part 1.-Formation of carbonate species on dehydroxylated CeO_2, at room temperature. *J. Chem. Soc. Faraday Trans.* **1989**, *85*, 929.
48. Li, C.; Sakata, Y.; Arai, T.; Domen, K.; Maruya, K.-i.; Onishi, T., Adsorption of carbon monoxide and carbon dioxide on cerium oxide studied by Fourier-transform infrared spectroscopy. Part 2.-Formation of formate species on partially reduced CeO_2 at room temperature. *J. Chem. Soc. Faraday Trans.* **1989**, *85*, 1451.
49. Binet, C.; Daturi, M.; Lavalley, J.-C., IR study of polycrystalline ceria properties in oxidised and reduced states. *Catal. Today* **1999**, *50*, 207.

50. Appel, L.; Eon, J.; Schmal, M., The CO_2-CeO_2 interaction and its role in the CeO_2 reactivity. *Catal. Lett.* **1998**, *56*, 199.
51. Yang, S.-C.; Su, W.-N.; Rick, J.; Lin, S. D.; Liu, J.-Y.; Pan, C.-J.; Lee, J.-F.; Hwang, B.-J., Oxygen Vacancy Engineering of Cerium Oxides for Carbon Dioxide Capture and Reduction. *ChemSusChem* **2013**, *6*, 1326.
52. Hahn, K. R.; Iannuzzi, M.; Seitsonen, A. P.; Hutter, J. r., Coverage Effect of the CO_2 Adsorption Mechanisms on CeO_2(111) by First Principles Analysis. *J. Phys. Chem. C* **2013**, *117*, 1701.
53. Reimers, W.; BaltanÃ¡s, M.; Branda, M., CO, CO_2 and H_2 adsorption on ZnO, CeO_2, and ZnO/CeO_2 surfaces: DFT simulations. *J. Mole. Mod.* **2013**, *20*, 1.
54. Cheng, Z.; Sherman, B. J.; Lo, C. S., Carbon dioxide activation and dissociation on ceria (110): A density functional theory study. *J. Chem. Phys.* **2013**, *138*, 014702.
55. Fujiki, J.; Yamada, H.; Yogo, K., Enhanced adsorption of carbon dioxide on surface-modified mesoporous silica-supported tetraethylenepentamine: Role of surface chemical structure. *Micropor. Mesopor. Mater.* **2015**, *215*, 76.
56. Mebane, D. S.; Kress, J. D.; Storlie, C. B.; Fauth, D. J.; Gray, M. L.; Li, K., Transport, Zwitterions, and the Role of Water for CO_2 Adsorption in Mesoporous Silica-Supported Amine Sorbents. *J. Phys. Chem. C* **2013**, *117*, 26617.
57. Gómez-García, M. A.; Pitchon, V.; Kiennemann, A., Pollution by nitrogen oxides: an approach to NO_x abatement by using sorbing catalytic materials. *Environ. Int.* **2005**, *31*, 445.
58. Ferrizz, R. M.; Egami, T.; Wong, G. S.; Vohs, J. M., Reaction of NO on CeO_2 and Rh/CeO_2 thin films supported on Al_2O_3(0 0 0 1) and YSZ(1 0 0). *Surf. Sci.* **2001**, *476*, 9.
59. Overbury, S. H.; Huntley, D. R.; Mullins, D. R.; Ailey, K. S.; Radulovic, P. V., Surface studies of model supported catalysts: NO adsorption on Rh/CeO_2(001). *J. Vac. Sci. Technol., A* **1997**, *15*, 1647.
60. Berner, U.; Schierbaum, K.; Jones, G.; Wincott, P.; Haq, S.; Thornton, G., Ultrathin ordered CeO_2 overlayers on Pt(111): interaction with NO_2, NO, H_2O and CO. *Surf. Sci.* **2000**, *467*, 201.
61. Mullins, D. R.; Overbury, S. H., Coverage dependent dissociation of NO on Rh supported on cerium oxide thin films. *Surf. Sci.* **2002**, *511*, L293.
62. Overbury, S. H.; Mullins, D. R.; Huntley, D. R.; Kundakovic, L., Chemisorption and Reaction of NO and N_2O on Oxidized and Reduced Ceria Surfaces Studied by Soft X-Ray Photoemission Spectroscopy and Desorption Spectroscopy. *J. Catal.* **1999**, *186*, 296.
63. Maitarad, P.; Zhang, D.; Gao, R.; Shi, L.; Li, H.; Huang, L.; Rungrotmongkol, T.; Zhang, J., Combination of Experimental and Theoretical Investigations of MnO_x/$Ce_{0.9}Zr_{0.1}O_2$ Nanorods for Selective Catalytic Reduction of NO with Ammonia. *J. Phys. Chem. C* **2013**, *117*, 9999.
64. Kawi, S.; Tang, Y. P.; Hidajat, K.; Yu, L. E. Synthesis and characterization of nanoscale CeO_2 catalyst for deNO_x, *J. Metastable Nanocrystal. Mater.* **2005**, *23*, 95.
65. Zhang, L.; Pierce, J.; Leung, V. L.; Wang, D.; Epling, W. S., Characterization of Ceria's Interaction with NO_x and NH_3. *J. Phys. Chem. C* **2013**, *117*, 8282.
66. Philipp, S.; Drochner, A.; Kunert, J.; Vogel, H.; Theis, J.; Lox, E. S., Investigation of NO adsorption and NO/O_2 co-adsorption on NO_x-storage-components by DRIFT-spectroscopy. *Top. Catal.* **2004**, *30-31*, 235.
67. Symalla, M. O.; Drochner, A.; Vogel, H.; Philipp, S.; GÃbel, U.; MÃller, W., IR-study of formation of nitrite and nitrate during NOx-adsorption on NSR-catalysts-compounds CeO_2 and BaO/CeO_2. *Top. Catal.* **2007**, *42-43*, 199.

68. Mihaylov, M. Y.; Ivanova, E. Z.; Aleksandrov, H. A.; Petkov, P. S.; Vayssilov, G. N.; Hadjiivanov, K. I., Formation of N_3^- during interaction of NO with reduced ceria. *Chem. Commun.* **2015**, *51*, 5668.
69. Azambre, B.; Zenboury, L.; Koch, A.; Weber, J. V., Adsorption and Desorption of NOx on Commercial Ceria-Zirconia ($Ce_xZr_{1-x}O_2$) Mixed Oxides: A Combined TGA, TPD-MS, and DRIFTS study. *J. Phys. Chem. C* **2009**, *113*, 13287.
70. Gao, X.; Jiang, Y.; Fu, Y.; Zhong, Y.; Luo, Z.; Cen, K., Preparation and characterization of CeO_2/TiO_2 catalysts for selective catalytic reduction of NO with NH_3. *Catal. Commun.* **2010**, *11*, 465.
71. Gao, X.; Jiang, Y.; Zhong, Y.; Luo, Z.; Cen, K., The activity and characterization of CeO_2-TiO_2 catalysts prepared by the sol-gel method for selective catalytic reduction of NO with NH_3. *J. Hazard. Mater.* **2010**, *174*, 734.
72. Chen, L.; Si, Z.; Wu, X.; Weng, D., DRIFT Study of CuO-CeO_2-TiO_2 Mixed Oxides for NO_x Reduction with NH_3 at Low Temperatures. *ACS Appl. Mater. Interfaces* **2014**, *6*, 8134.
73. Ma, Z.; Weng, D.; Wu, X.; Si, Z., Effects of WO_x modification on the activity, adsorption and redox properties of CeO_2 catalyst for NO_x reduction with ammonia. *J. Environ. Sci.* **2012**, *24*, 1305.
74. Chen, L.; Li, J.; Ablikim, W.; Wang, J.; Chang, H.; Ma, L.; Xu, J.; Ge, M.; Arandiyan, H., CeO_2-WO_3 Mixed Oxides for the Selective Catalytic Reduction of NO_x by NH_3 Over a Wide Temperature Range. *Catal. Lett.* **2011**, *141*, 1859.
75. Chen, L.; Li, J.; Ge, M., DRIFT Study on Cerium-Tungsten/Titiania Catalyst for Selective Catalytic Reduction of NO_x with NH_3. *Environ. Sci. Tech.* **2010**, *44*, 9590.
76. Chen, L.; Li, J.; Ge, M.; Zhu, R., Enhanced activity of tungsten modified CeO_2/TiO_2 for selective catalytic reduction of NO_x with ammonia. *Catal. Today* **2010**, *153*, 77.
77. Daturi, M.; Bion, N.; Saussey, J.; Lavalley, J. C.; Hedouin, C.; Seguelong, T.; Blanchard, G., Evidence of a lacunar mechanism for deNO activity in ceria-based catalysts. *Phys. Chem. Chem. Phys.* **2001**, *3*, 252.
78. Ilieva, L.; Pantaleo, G.; Ivanov, I.; Venezia, A. M.; Andreeva, D., Gold catalysts supported on CeO_2 and CeO_2-Al_2O_3 for NO_x reduction by CO. *Appl. Catal. B: Environ.* **2006**, *65*, 101.
79. Ilieva-Gencheva, L.; Pantaleo, G.; Mintcheva, N.; Ivanov, I.; Venezia, A. M.; Andreeva, D., Nano-structured gold catalysts supported on CeO_2 and CeO_2-Al_2O_3 for NO_x reduction by CO: effect of catalyst pretreatment and feed composition. *J. Nanosci. Nanotech.* **2008**, *8*, 867.
80. Machida, M., NO_x-Sorbing Metal Oxides, MnO_x-CeO_2. Oxidative NO Adsorption and NO_x-H_2 Reaction. *Catal. Surv. Japan* **2002**, *5*, 91.
81. Chang, H.; Chen, X.; Li, J.; Ma, L.; Wang, C.; Liu, C.; Schwank, J. W.; Hao, J., Improvement of Activity and SO_2 Tolerance of Sn-Modified MnOx-CeO_2 Catalysts for NH_3-SCR at Low Temperatures. *Environ. Sci. Tech.* **2012**, *47*, 5294.
82. Wang, Y.; Ge, C.; Zhan, L.; Li, C.; Qiao, W.; Ling, L., MnO_x-CeO_2/Activated Carbon Honeycomb Catalyst for Selective Catalytic Reduction of NO with NH_3 at Low Temperatures. *Ind. Eng. Chem. Res.* **2012**, *51*, 11667.
83. Machida, M.; Kurogi, D.; Kijima, T., MnO_x-CeO_2 Binary Oxides for Catalytic NO_x-Sorption at Low Temperatures. Selective Reduction of Sorbed NO_x. *Chem. Mater.* **2000**, *12*, 3165.
84. Machida, M.; Uto, M.; Kurogi, D.; Kijima, T., MnO_x-CeO_2 Binary Oxides for Catalytic NO_x Sorption at Low Temperatures. Sorptive Removal of NO_x. *Chem. Mater.* **2000**, *12*, 3158.

85. Costa, C. N.; Efstathiou, A. M., Mechanistic Aspects of the H_2-SCR of NO on a Novel Pt/MgO-CeO_2 Catalyst. *J. Phys. Chem. C* **2007**, *111*, 3010.
86. Machida, M., NO_x-Sorbing Metal Oxides, MnO_x-CeO_2. Oxidative NO Adsorption and NO_x-H_2 Reaction. *Catal. Surv. Japan* **2002**, *5*, 91.
87. Rodriguez, J. A.; Jirsak, T.; Sambasivan, S.; Fischer, D.; Maiti, A., Chemistry of NO_2 on CeO_2 and MgO: Experimental and theoretical studies on the formation of NO_3. *J. Chem. Phys.* **2000**, *112*, 9929.
88. Yang, Z.; Woo, T. K.; Hermansson, K., Adsorption of NO on unreduced and reduced CeO_2 surfaces: A plane-wave DFT study. *Surf. Sci.* **2006**, *600*, 4953.
89. Zhang, J.; Gong, X.-Q.; Lu, G., A DFT + U study of NO evolution at reduced CeO_2(110). *Phys. Chem. Chem. Phys.* **2014**, *16*, 16904.
90. Nolan, M.; Parker, S. C.; Watson, G. W., Reduction of NO_2 on Ceria Surfaces. *J. Phys. Chem. B* **2006**, *110*, 2256.
91. Overbury, S. H.; Mullins, D. R.; Huntley, D. R.; Kundakovic, L., Chemisorption and Reaction of Sulfur Dioxide with Oxidized and Reduced Ceria Surfaces. *J. Phys. Chem. B* **1999**, *103*, 11308.
92. Waqif, M.; Bazin, P.; Saur, O.; Lavalley, J. C.; Blanchard, G.; Touret, O., Study of ceria sulfation. *Appl. Catal. B: Environ.* **1997**, *11*, 193.
93. Ferrizz, R. M.; Gorte, R. J.; Vohs, J. M., TPD and XPS Investigation of the Interaction of SO_2 with Model Ceria Catalysts. *Catal. Lett.* **2002**, *82*, 123.
94. Flouty, R.; Abi Aad, E.; Siffert, S.; Aboukais, A.; Aboukaïs, A., Formation of cereous sulphate phase upon interaction of SO_2 with ceria at room temperature - Thermal analysis, Raman and EPR study. *J. Therm. Anal. Calorim.* **2003**, *73*, 727.
95. Smirnov, M. Y.; Kalinkin, A. V.; Pashis, A. V.; Prosvirin, I. P.; Bukhtiyarov, V. I., Interaction of SO_2 with Pt Model Supported Catalysts Studied by XPS. *J. Phys. Chem. C* **2014**, *118*, 22120.
96. Smirnov, M. Y.; Kalinkin, A. V.; Pashis, A. V.; Sorokin, A. M.; Noskov, A. S.; Bukhtiyarov, V. I.; Kharas, K. C.; Rodkin, M. A., Comparative XPS Study of Al_2O_3 and CeO_2 Sulfation in Reactions with SO_2, SO_2 + O_2, SO_2 + H_2O, and SO2 + O_2 + H_2O. *Kinet. Catal.* **2003**, *44*, 575.
97. Smirnov, M. Y.; Kalinkin, A. V.; Pashis, A. V.; Sorokin, A. M.; Noskov, A. S.; Kharas, K. C.; Bukhtiyarov, V. I., Interaction of Al_2O_3 and CeO_2 Surfaces with SO_2 and SO_2 + O_2 Studied by X-ray Photoelectron Spectroscopy. *J. Phys. Chem. B* **2005**, *109*, 11712.
98. Happel, M.; Lykhach, Y.; Tsud, N.; SkÃ¡la, T. Å.; Prince, K. C.; MatolÃn, V.; Libuda, J. r., Mechanism of Sulfur Poisoning and Storage: Adsorption and Reaction of SO_2 with Stoichiometric and Reduced Ceria Films on Cu(111). *J. Phys. Chem. C* **2010**, *115*, 19872.
99. Happel, M.; Lykhach, Y.; Tsud, N.; SkÃ¡la, T. Å.; JohÃ¡nek, V.; Prince, K. C.; MatolÃn, V.; Libuda, J. r., SO_2 Decomposition on Pt/CeO_2(111) Model Catalysts: On the Reaction Mechanism and the Influence of H_2 and CO. *J. Phys. Chem. C* **2012**, *116*, 10959.
100. Rodriguez, J.; Rodriguez, T.; Jirsak, A.; Freitag, J.; Hanson, J.; Larese, S.; Chaturvedi, Interaction of SO_2 with CeO_2 and Cu/CeO_2 catalysts: photoemission, XANES and TPD studies. *Catal. Lett.* **1999**, *62*, 113.
101. Tumuluri, U.; Li, M.; Cook, B. G.; Sumpter, B.; Dai, S.; Wu, Z., Surface Structure Dependence of SO_2 Interaction with Ceria Nanocrystals with Well-Defined Surface Facets. *J. Phys. Chem. C* **2015**, *119*, 28895.

102. Waqif, M.; Saad, A. M.; Bensitel, M.; Bachelier, J.; Saur, O.; Lavalley, J.-C., Comparative study of SO_2 adsorption on metal oxides. *J. Chem. Soc. Faraday Trans.* **1992**, *88*, 2931.
103. Bazin, P.; Saur, O.; Lavalley, J. C.; Blanchard, G.; Visciglio, V.; Touret, O., Influence of platinum on ceria sulfation. *Appl. Catal. B: Environ.* **1997**, *13*, 265.
104. Lavalley, J. C., Infrared spectrometric studies of the surface basicity of metal oxides and zeolites using adsorbed probe molecules. *Catal. Today* **1996**, *27*, 377.
105. Luo, T.; Vohs, J. M.; Gorte, R. J., An Examination of Sulfur Poisoning on Pd/Ceria Catalysts. *J. Catal.* **2002**, *210*, 397.
106. Twu, J.; Chuang, C. J.; Chang, K. I.; Yang, C. H.; Chen, K. H., Raman spectroscopic studies on the sulfation of cerium oxide. *Appl. Catal. B: Environ.* **1997**, *12*, 309.
107. Jiang, L.; Wei, M.; Xu, X.; Lin, Y.; LÃ¼, Z.; Song, J.; Duan, X., SO_x Oxidation and Adsorption by CeO_2/MgO: Synergistic Effect between CeO_2 and MgO in the Fluid Catalytic Cracking Process. *Ind. Eng. Chem. Res.* **2011**, *50*, 4398.
108. Luo, T.; Gorte, R. J., Characterization of SO_2-poisoned ceria-zirconia mixed oxides. *Appl. Catal. B: Environ.* **2004**, *53*, 77.
109. Yu, Q.; Zhang, S.; Wang, X.; Zhang, J.; Lu, Z., Study on Sulfation of CeO_2/Al_2O_3 Sorbent in Simulated Flue Gas. *Rare Earths* **2007**, *25*, 184.
110. Lu, Z.; Müller, C.; Yang, Z.; Hermansson, K.; Kullgren, J., SO_x on ceria from adsorbed SO_2. *J. Chem. Phys.* **2011**, *134*, 184703.
111. Lu, Z.; Kullgren, J.; Yang, Z.; Hermansson, K., Sulfidation of Ceria Surfaces from Sulfur and Sulfur Diffusion. *J. Phys. Chem. C* **2012**, *116*, 8417.
112. Kullgren, J.; Lu, Z.; Yang, Z.; Hermansson, K., Sulfidation and Sulfur Recovery from SO_2 over Ceria. *J. Phys. Chem. C* **2014**, *118*, 17499.
113. Liu, Y.; Cen, W.; Wu, Z.; Weng, X.; Wang, H., SO_2 Poisoning Structures and the Effects on Pure and Mn Doped CeO_2: A First Principles Investigation. *J. Phys. Chem. C* **2012**, *116*, 22930.
114. Nolan, M.; Watson, G. W., The Surface Dependence of CO Adsorption on Ceria. *J. Phys. Chem. B* **2006**, *110*, 16600.
115. Nolan, M.; Parker, S. C.; Watson, G. W., The electronic structure of oxygen vacancy defects at the low index surfaces of ceria. *Surf. Sci.* **2005**, *595*, 223.
116. Kandemir, T.; Girgsdies, F.; Hansen, T. C.; Liss, K.-D.; Kasatkin, I.; Kunkes, E. L.; Wowsnick, G.; Jacobsen, N.; Schlögl, R.; Behrens, M., In Situ Study of Catalytic Processes: Neutron Diffraction of a Methanol Synthesis Catalyst at Industrially Relevant Pressure. *Angew. Chem. Int. Ed.* **2013**, *52*, 5166.
117. Mamontov, E.; Egami, T., Structural defects in a nano-scale powder of CeO_2 studied by pulsed neutron diffraction. *J. Phys. Chem. Solids* **2000**, *61*, 1345.
118. Kümmerle, E. A.; Heger, G., The Structures of C-$Ce_2O_{3+\delta}$, Ce_7O_{12}, and $Ce_{11}O_{20}$. *J. Solid State Chem.* **1999**, *147*, 485.

TOC: